RESEARCH ARTICLE OPEN ACCESS

Energy Conversion on Differential Magnetization of Fe_3O_4 Ferrofluid

S. D. Kemkar *, Milind Vaidya **, Dipak Pinjari***, Chandrakant Holkar****, Sanjana Kemkar*****, Siddhesh Nanaware******, Sanjukta Kemkar*******

*Department of Physics, Smt. Chandibai Himathmal Mansukhani College, Ulhasnagar, India.
**Department of Physics, Vedanta College , Vithalwadi, India
***Department of Chemical Engineering, Institute of Chemical Technology, Mumbai, India
****Department of Chemical Engineering, Institute of Chemical Technology, Mumbai, India
*****Smolensk State Medical University, Smolensk, Russia
******STES NBN Sinhgad School of Engineering, Pune, India
*******Department of Microbiology, Smt. CHM College, Ulhasnagar, India

ABSTRACT
Ferrofluids are stable suspension of ferrimagnetic nanoparticles in hydrocarbon carrier. This fluid is used for harvesting energy using energy conversion device which is presented in this work. The device consists of two chambers, they are hot and cold chamber in which differential magnetization is linked with an inductor. Classically very small value of coupling coefficient |k| has been observed. System configuration shows an emf generation rate of about 44.4μV/K. Presented work shows another way of harvesting energy. Ferrofluid having a particle size of 21nm was used in this case.

Keywords: Magnetic nanoparticles; energy generation; energy harvesting; magnetite; ferrofluids; Fe_3O_4.

I. INTRODUCTION

The process of deriving energy from various energy sources like wind, solar, temperature, vibration, etc with the help of energy harvesting devices are well known to us. Energy harvesters provide a very small amount of power with low degree of efficiency. Some vibrational sources in the environment include electric motor-rotation, wind motion, wave motion, vehicle motion and human movement, all of which vary widely in both frequencies as well as amplitude [1]. Vibrational energy can be harvested using several methods, such as, piezoelectric, electrostatic and electromagnetic transduction. Electromagnetic energy harvesters are better candidates for low frequency vibrations, but, their peak output voltage is relatively low. In addition, the design of the applied power electronics and electromagnetic systems in the devices are crucial in efficiently delivering the harvested power to the load. Harvester configuration has been studied with the basic concept remaining the same. The core principle is that the vibrations of magnetic field is linked as per Faraday's law to induce a current which can then drive an electrical device [2]. Ferrofluids have attracting application in various fields like automobiles, electrical engineering [28,30,31,32], space technology, computer science, medical imaging, biomedical [3,4], targeted drug delivery [5,6], optical fiber [27,29] and sensors [7,8] etc. The temperature sensitivity issue on ferrofluid has already been studied [9,10]. Attempts have been made for generating energy from ferrofluids whereas, micro devices are used for fabrication and generation of energy.

Presented work investigates a magnetic fluid based electromagnetic energy harvester as a macro device. The generation of energy using magnetic field was observed by inducing Electromotive Force (emf) in a coil due to oscillating nature of the magnetic nanoparticles in ferrofluid [11]. Ferrofluids are colloidal liquids made up of nanoscale permanent magnetic dipoles, can change shape freely and has ability to generate an electromotive force (emf) from small vibrations. Ferrofluids are often applied to energy harvesting devices, because they have fluidity, magnetic properties and behaves like soft ferromagnetic substance [12]. Study of flow analysis of ferrofluids, magnetic circuit and characteristics of resultant magnetic system is carried out classically. An energy harvester model based on magnetic field generated by a ferrofluid is proposed and developed. Thereafter, the feasibility of the proposed method is shown and its emf characteristics have been discussed with reference to experimental data.

In consequence, the aim of this work is to develop an energy conversion device using a differential magnetization of Fe_3O_4 based Ferrofluid. The characterizations of the synthesized nanoparticles were carried out with TEM, VSM and XRD techniques. Vibrational energy from thermal

agitation is used as a main source to generate small amount of electrical energy.

II. MATERIALS AND METHOD

2.1 Materials

Ferric chloride hexahydrate ($FeCl_3{:}6H_2O$, >99%), ferrous chloride tetrahydrate ($FeCl_2{:}4H_2O$, >99%), hydrochloric acid (HCl, >37%), Oleic acid $C_{18}H_{34}O_2$ (anionic surfactant) and ammonia were obtained from Sigma Aldrich. Milli-Q water was re-deionized (specific conductance < 0.1 s/cm) and deoxygenated by bubbling with N_2 gas for 1hr prior to use.

2.2 Preparation of Fe_3O_4 Nanoparticles

Co-precipitation method was used for the preparation of magnetite Fe_3O_4 nanoparticles . Stock solutions of 1.28M $FeCl_3{:}6H_2O$, 0.64M $FeCl_2{:}4H_2O$ were prepared as a source of iron by dissolving the respective chemicals in Milli-Q water under vigorous stirring. Stock solution of 1.5M NH_4OH was prepared. A solution of 0.01M HCl was prepared for surface neutralization. 25 ml of iron source was added drop-wise into 250 ml of alkali source under vigorous mechanical stirring for 30 minutes at 90°C. N_2 gas was passed through the reaction medium during synthesis operation in a closed system. When ammonium hydroxide reacts with solution, then forms ferric hydroxide and ferrous hydroxide. Oxidation process has taken place immediately giving out FeO and Fe_2O_3 molecules. Ferritisation process has been followed and final product of Fe_3O_4 was prepared. The precipitated powder was black in color and this has indicated the formation of Fe_3O_4. For the preparation of Fe_3O_4 nanoparticles, the concentration of Fe^{2+} and Fe^{3+} ions must be 1:2 respectively. In the same way, aqueous dispersion of magnetic nanoparticles were prepared by alkalinizing an aqueous mixture of ferric and ferrous salts with ammonia at room temperature [6], while a solution of 1.5M sodium oleate $C_{18}H_{33}O_2Na$(surfactant) at pH = 9.4 was prepared. Coating on the nano particles was carried out using Na-oleate under vigorous mechanical stirring for further 30 minutes at 90°C to acquire steric repulsion.

$Fe_3O_4 + C_{17}H_{33}COONa \longrightarrow [Fe_3O_4.C_{17}H_{33}COO^-]$ (Anionic Na-oleate adsorbed particle particle)

After coating, the surfactant which was adsorbed physically on the surface of the particles and excess surfactant was removed by washing with deoxygenated Milli-Q water. Centrifugation and peptizing the solution was carried out three times. After washing the powder 4 times, the precipitated powder was isolated by applying an mild external magnetic field and the supernatant was removed from the precipitate by decantation. The color of the powder was changed to brown from black after coating of surfactant. Deoxygenated Milli-Q water was added to wash the powder and the solution was decanted after centrifugation at 3500rpm. The excess of Cl^- ions was detected by addition of Ag^+ ions. The chemical reaction of Fe_3O_4 precipitation was carried out as follows [13,14] -:

$$FeCl_2+2[FeCl_3]+8[NH_4OH] \longrightarrow Fe_3O_4+8[NH_4Cl]+4[H_2O]$$

$$2[NH_4OH] + FeCl_2 \longrightarrow 2[NH_4Cl] + Fe(OH)_2$$

$$2[3NH_4OH] + 2[FeCl_3] \longrightarrow 2[3NH_4Cl]+ 2[Fe(OH)_3]$$

$$Fe(OH)_2 \longrightarrow FeO+H_2O$$

$$2\,Fe(OH)_3 \longrightarrow Fe_2O_3 + 3\,H_2O$$

$$FeO + Fe_2O_3 \longrightarrow FeO.Fe_2O_3 = Fe_3O_4$$

The principle reaction was as follow:

$$Fe^{2+} + 2Fe^{3+} + 8OH^- \xrightarrow{\text{pH 8.5}} Fe_3O_4 + 4\,H_2O$$

When reaction proceeded, pH of the reaction was controlled with the help of buffer solution. A complete precipitation of Fe_3O_4 was achieved between pH = 7.5-14, while maintaining a molar ratio of Fe^{2+} : Fe^{3+} = 1:2 under a non-oxidizing environment.

Shiny magnetic powder obtained was washed with ethanol and dried in the oven at 80°C. All the characterizations of the sample were done in solid phase.

The size of the single domain particle depends on the compound and different anisotropic energy terms. The critical radius r_c below which a particle acts as a single domain particle is given by equation-1 [25].

$$r_c \approx 9\left[\frac{(AK_\mu)^{1/2}}{\mu_o M_s^2}\right] \qquad (1)$$

Where, K_μ= Uniaxial Anisotropic Constant

A = Exchange Constant

M_s= Saturation Magnetization

μ_o = Permeability of free space

2.3Fe_3O_4 based Ferrofluid

The powder prepared was dispersed in kerosene which is a hydrocarbon carrier. Surfactant was used for stability of ferrofluid against agglomeration. Ferrofluid with 2.5% volumetric

concentration was prepared. The preparation of ferrofluid can also be seen elsewhere [15].

2.4 Functional Diagram for Electromagnetic Energy Harvester using Fe_3O_4 Ferrofluid

Fig-1 shows a diagram of the proposed energy harvester using a ferrofluid with coil in its core. This energy harvester consists of two boxes. One box is water cooling chamber and other box is divided into two sub chambers called hot chamber and cold chamber. The partition of the chambers has a semi circular hole at the top as well as at the bottom. The water cooling box is attached at the upper side of the cold chamber and it acts as a cooling reservoir. A cooling reservoir has the dimensions of 25mm x 25mm x 75mm. The dimension of main box is 25mm x 25mm x 75mm with partition at 12.5mm from the edge. One side of the copper metallic plate is connected at the end of the bottom of hot chamber and the other side of metallic plate is kept open for heat input.

Figure 1.a) Prototype macro cell used for energy generation.

Hot and cold sub chambers were filled up with ferrofluid having 2.5% volume concentration. Nanoparticles are a ferrimagnetic particle with diameters of order 21nm as such particles behaves as a single domain magnetic particle.

The energy generating coil was placed exactly at the center of the main box assembly having 25,000 turns of 42 SWG and wounded on Bakelite former having 15mm width with diameter of 103mm. The entire assembly was housed in a vertical static magnetic field of 1Tesla as shown in Fig-1 denoting functional block. When heat input is given to the copper plate, it conducts and transfers it to the bottom of the hot chamber. Ferrofluid liquid which is present in hot chamber gets heated up and flows in upward direction due to natural convection.

Further, it moves in to the upper side of the cold chamber. The water cooling chamber which is connected at the top of cold chamber helps to cool the hot ferrofluid entering the cold chamber. The ferrofluid enters the cold chamber and flows in the downward direction; it reaches at the bottom of the partition of the cold chamber. It then gets transferred to the hot chamber from bottom opening. Again ferrofluid gets heated up and the whole process is repeated again and again.

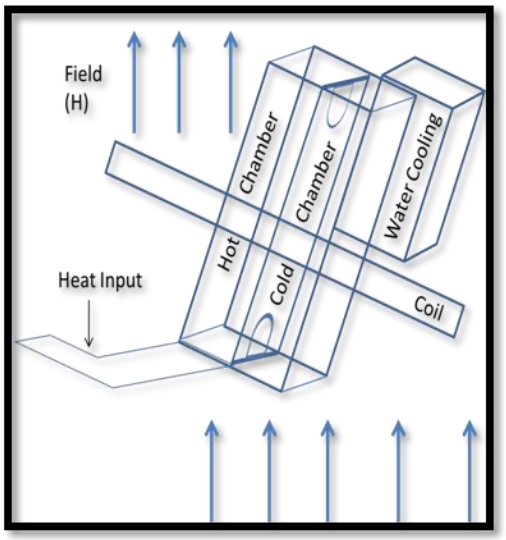

Figure 1.b) Functional block diagram for energy generation setup, using ferrofluid.

Thus, the natural convection causes the ferrofluid to move in the container. This motion of the ferrofluid changes the magnetic flux generated by the permanent magnet and creates a time-varying fluctuations in magnetic field, depending upon the temperature. This field induces an EMF in the coil, thus generating small electric potential. The output of coil was attached to oscilloscope (HAMEG / HM407-2) and readings were taken at different temperatures from 300K to 318K. Smaller range in temperature was selected for the device expected to work near room temperature.

III. CHARACTERIZATION OF Fe_3O_4 NANOPARTICLES

Prepared Fe_3O_4 powder was characterized by using Phillips PW 1800 powder X-ray diffractometer. Scanning range during characterization was taken between 6-80^O. The morphology and particle size of these nanoparticles was characterized by TEM model H-7650 using

accelerating voltage of 120KV. The resultant emf generated in induction coil was in the range of few mV and discussed later.

IV. RESULTS AND DISCUSSION

4.1 TEM and XRD of Fe_3O_4 Nanoparticles

The TEM of the powder is shown in the Fig-2. (JEOL make Model-JEM 2100). Evacuation current is required to be below 64 micro amps for TEM to work under safety limits. All images have been taken below 32 micro amps in safe limit for the filament of TEM.

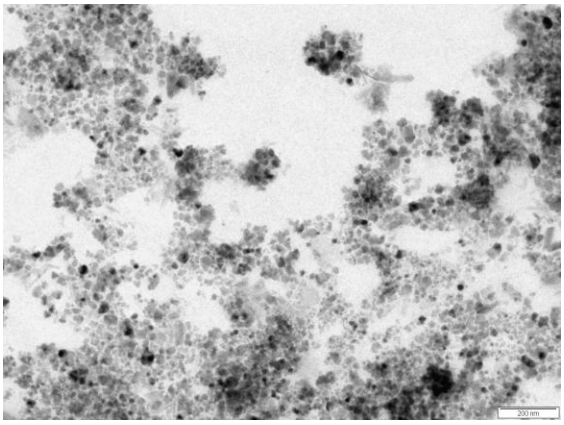

Figure 2. TEM image of Fe_3O_4 ferrofluid having average particle size of 21nm.

At this limit the beam voltage was set at 200KV and the peak beam current of 98 micro amps was observed. During image extraction, it is observed that 3 to 4 micro amps of beam current have been increased. TEM image shows the size of nanoparticles around 21nm.

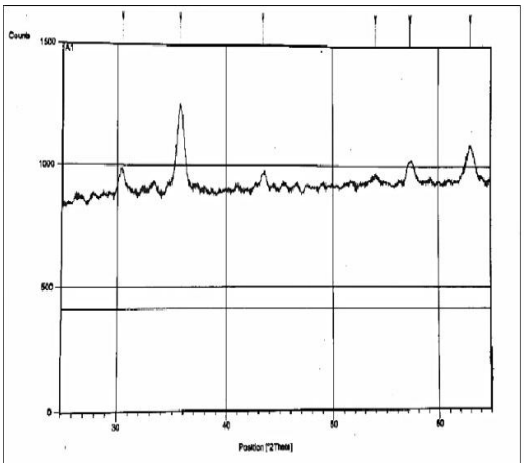

Figure 3. XRD pattern of Fe_3O_4 powder

Magnetite powder was dried in oven for 24Hrs at 80^OC. The structural properties of particles were analyzed by XRD (Philips make /X'pert PRO model) as shown in Fig-3. The size of the crystal cluster was calculated by Scherrer's formula as in equation 2. Wavelength λ of source was taken 0.15406nm .

$$D = K\lambda/(B\cos\theta) \quad (2)$$

B is a full width half maximum (FWHM), K is the shape parameter and θ is the bragg's angle. The value of K is 0.89 for magnetite. The largest intensity in the graph is at [311] plane with 2θ of 35.7^o. Half maximum intensity width of the peak accounted with instrument broadening; particle size was calculated to 20.7nm.

4.2 Magnetization of Fe_3O_4 Powder

Magnetization of the magnetite powder is as shown in Fig-4. The saturation magnetization of 21nm magnetite particle was observed as 80.2emu/cc at 300K and the applied field was 10kG.

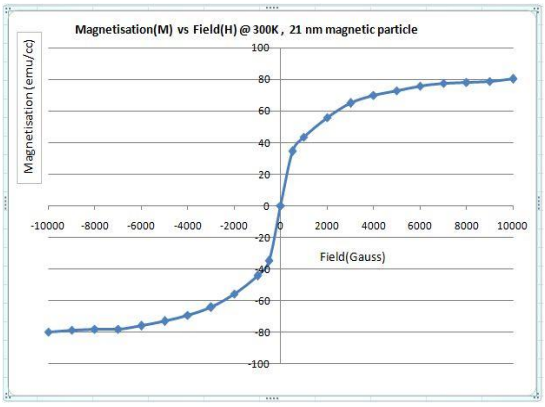

Figure 4. Magnetization (emu/cc) vs field (Gauss) at 300K performed on 21 nm size Fe_3O_4 nanoparticle.

4.3 Thermal effect on Ferrofluid and Induced Electromotive Force

Ferrofluids which are subjected to static uniform magnetic field and thermal gradient have interesting phenomena, which leads to thermomagnetophoretic mobility in ferrofluids. Thermomagnetophoretic mobility is a kind of thermo diffusion as well as self oscillatory convection and the effect is called as Soret Effect. This is characterized by Soret Coefficient S_T. The soret coefficient has been introduced in such a way that, if the particles tend to concentrate in the hottest region, then the soret coefficient is negative ($S_T < 0$); this is thermophilic behavior and if the particles of ferrofluid tend to go away from the hottest region, then the soret coefficient is positive ($S_T > 0$); this is thermophobic behavior. In current system, the value of Soret coefficient lies in the range from 0.001 /K to 1.0 /K. It is also reported that Soret Coefficient S_T is also a function of Volume Fraction[16,17]. The Marangoni effect also called as the Gibbs–Marangoni effect, is the mass transfer along an interface between two fluids due to surface tension

gradient. In the case of temperature dependence, this phenomenon is called as thermo-capillary convection or Benard–Marangoni convection. Since a liquid with a high surface tension have pull more strongly on the surrounding liquid than the one with a low surface tension. The presence of a gradient in surface tension will naturally cause the liquid to flow away from regions of low surface tension. The surface tension gradient can be caused by concentration gradient or by a temperature gradient due to the fact that the surface tension is also a function of temperature[18,19].

Thus, the temperature gradient causes the motion of flowing of ferrofluid in the container. This motion of the ferrofluid in the container make changes in the magnetic flux of permanent magnet and creates a time-varying magnetic flux depending upon the temperature fluctuations. This flux induces an emf in a coil. The output of coil has benn shown graphically as Fig-5.

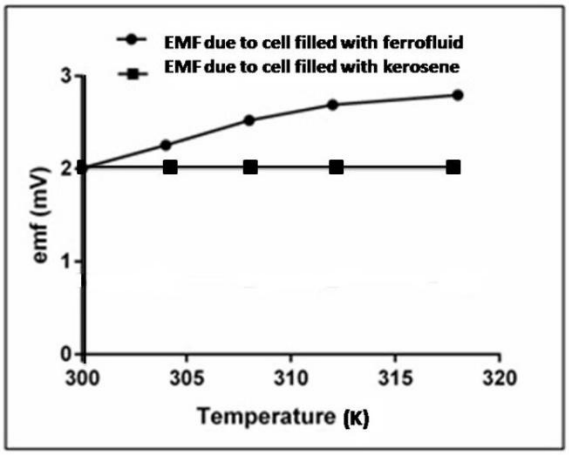

Figure 5. Rise in differentially generated emf (mV) vs Temp (K)

Temperature of copper plate was raised from 300K to 318K whereas voltage observed from 300K to 318K was from 2.0 mV to 2.8 mV..

V. THEORETICAL ANALYSIS

5.1 Analysis of coupling coefficient |K|

Super-paramagnetic iron oxide nanoparticles show unique magnetic properties. The saturation magnetization, M_{smsd} of individual single domain magnetic nanoparticle of specific size represents the maximum magnetization (A/m) that a particle can experience.

$$M_{smsd} = m_p M_d \left[\left(\frac{r-\delta}{r}\right)^3\right] \qquad (3)$$

Where,

m_p is the mass of the individual particle,

M_d is the bulk saturation magnetization (A/m/g),

r is the radius of the particle

$\boldsymbol{\delta}$ is non-magnetic thickness of shell over core of the particle.

Thickness of the shell is about 1nm for super-paramagnetic particle sizes (Milliner al. 2007). With the help of M_{smsd}, it is possible to find spontaneous magnetization, M_{spont} which is present in magnetic nanoparticle without applying any external magnetic field. This is also an ordered magnetization in a particle[20].

$$M_{spont} = M_{smsd}\left[1 - 0.3\left(\frac{T}{T_c}\right)^{1.2}\right] \qquad (4)$$

T is the temperature of a nanoparticle and T_c is Curie temperature of bulk materials. At temperatures above Curie temperatureT_c, the materials do not have ordered magnetic domain and thus shows no spontaneous magnetization. The validity of this relationship is observed for maghemite [Fe_2O_3] up to a temperature of 0.5 T_c [21]. T_c for maghemite is 685 K therefore establishing 340K as a maximum valid temperature as far as this model is concerned. Other dimensionless important quantity to consider is χ_p, susceptibility of magnetic nanoparticle and it is deduced from equation-5. Susceptibility of the magnetic nanoparticle depends on the volume of the particle V_p , temperature T as well as spontaneous magnetization M_{spont}, k is Boltzman's constant, μ_0 is free space permeability.

$$\chi_p = {M_{spont}}^2 \left[\frac{\mu_0 V_p}{3kT}\right] \qquad (5)$$

It is the quantity which describes the magnetic response to an applied magnetic field. Generally, value is complex in nature at low temperatures below 150 K as well as complex non-linear behavior at dynamic magnetic fields[22]. On these assumptions, magnetite nanoparticles too are subjected to the temperature below 340K such that the above model describing equations 1-3 are applicable.

Particle in colloidal ferrofluid with its magnetic moments m (A-m^2) are analogous to the molecules of paramagnetic gas. In the absence of externally applied magnetic field, the particles are randomly oriented and colloidal ferrofluid has no net magnetization. In ordinary magnetic field strength, the tendency of dipole moments to align to an external magnetic field is partially overcome by thermal agitation. Particles align more and more if

strength of externally applied magnetic field is increased. Under extremely high magnetic field strength the particles may completely align and the magnetization achieved for colloidal ferrofluid is at its saturation value. Langevin's classical theory is applied to give a superparamagnetic relationship on the assumption that there is a negligible particle-particle magnetic interaction. Consider a cylindrical small volume of magnetically polarized colloidal ferrofluid subjected to external magnetic field $\mathbf{H}_o$ with gradient $\delta\mathbf{H}_o$ and poles of density $\mu_o M$ (scalar) appearing at extreme ends of the cylindrical elements of volume δV. These poles of density ρ (poles/m^2) appear equal in numbers and opposite polarity at extreme ends of the cylindrical elements. Area A_c is considered as a cross sectional area at extreme ends of the cylindrical element and d (scalar) is an axial length of the cylindrical element. **M** is a magnetization vector aligned with the geometrical axis of a cylindrical elemental volume and collinear in the direction of applied magnetic field gradient. Whereas $\delta\mathbf{H}_o$ is a change in $\mathbf{H}_o$ in the direction of geometric axis of the subjected cylindrical volume element. Applied field $\mathbf{H}_o$ may be taken as a force on a unit pole and hence the force experienced by the volume element is-

$\mathbf{H}_o\ \rho\ A_c + (\mathbf{H}_o + \delta\mathbf{H}_o)\ \rho\ A_c = \delta\mathbf{H}_o\ \rho\ A_c$

$\delta\mathbf{H}_o = (\mathbf{d}.\nabla)\ \mathbf{H}_o$ whereas, **d** is axial displacement vector. $(\mathbf{d}.\nabla)\ \mathbf{H}_o = (d/M)(\mathbf{M}.\nabla)\mathbf{H}_o$ and force density, $\mathbf{F} = \mu_o\ (\mathbf{M}\ .\ \nabla)\ \mathbf{H}_o$ with $\mu_o\mathbf{M}$ represent the vector moment per unit volume. Dipole moment for volume element is $md = \rho\ A_c d = \mu_o\mathbf{M}\ A_c d$, where $\rho = \mu_o\mathbf{M}$ and $A_c d$ is volume δV of element, therefore $\mathbf{m}_d = \mu_o\mathbf{M}\delta\mathbf{V}$. Vector dipole moment $\mathbf{m}_d$ is in the direction of displacement vector **d**.

Now, torque $\delta\mathbf{T}$ acting on volume element on application of uniform magnetic field is considered when $\delta\mathbf{H}_o = 0$, under no magnetic field gradient applied to vector dipole moment is given as-

$\delta\mathbf{T} = \mathbf{m}_d \times \mathbf{H}_o = \mu_o\mathbf{M}\ \delta\mathbf{V} \times \mathbf{H}_o$

Torque per unit volume $= \delta\mathbf{T}/\ \delta\mathbf{V} = (\mu_o\mathbf{M}\ \delta\mathbf{V} \times \mathbf{H}_o) / \delta\mathbf{V} = (\mu_o\mathbf{M} \times \mathbf{H}_o)$ is a torque density. This expression is independent of the choice of origin of the co-ordinate system. For soft magnetic solid material in colloidal ferrofluid, **M** is parallel to $\mathbf{H}_o$. This saturation magnetization of purely ferromagnetic solid material is called domain magnetization M_d. Generally speaking of hard magnetic material shows hysteresis whereas soft magnetic material does not show or show very less hysteresis. For soft material the force density reduces to $\mu_o M\nabla\mathbf{H}_o$ as vector **M** has no different direction than $\mathbf{H}_o$. Therefore, work per unit volume = **force density.** $\mathbf{d}_s = \mu_o M(\nabla\mathbf{H}_o).\mathbf{d}_s = \mu_o M dH/ds$ Rosensweig R. E. has extensively evaluated concerned dynamics in 1985.

Other important property of colloidal ferrofluid is susceptibility and is a standard ratio as shown in equation-6.

$$\chi = \frac{M}{H} \tag{6}$$

Equation (5) has been replaced in equation (4) and rewritten as equation (7)

$$\chi = \frac{M}{H} = M_{smsd}{}^2 \left[1 - 0.3\left(\frac{T}{T_c}\right)^{1.2}\right]^2 \left[\frac{\mu_o V_p}{3kT}\right] \tag{7}$$

Since,

$$B = \mu_0.H$$
$$H = \frac{B}{\mu_0} \tag{8}$$
$$M = M_{spont} \text{ for particle.}$$

Replacing above H and M and in equation (6) we get equation (8) as follows.

$$\frac{\mu_o M_{spont}}{B} = M_{smsd}{}^2 \left[1 - 0.3\left(\frac{T}{T_c}\right)^{1.2}\right]^2 \left[\frac{\mu_o V_p}{3kT}\right] \tag{9}$$

Expanding, we get B_p wb/m^2 magnetic field density at particle.

$B = B_p$ is a magnetic flux density (wb/m^2) of a particle. Replacing B as well as M_{spont} from equation-4 in to equation-9 and solving for B_p, we get equation-10

$$B_p = \frac{3\,kT}{V_p.M_{smsd}\left[1-0.3\left(\frac{T}{T_c}\right)^{1.2}\right]}\ wb/m^2 \tag{10}$$

In ferrofluid for control sample within the core of a coil i.e. a-b-c-d-e-f-a as per Fig-7,

$$n_s = \frac{\mu_o M_s}{\bar{m}} \tag{11}$$

Where $\bar{m}$ is average magnetic moment per particle in A-m^2 in the direction of applied magnetic field and M_s is saturation magnetization of ferrofluid in A/m, n_s particles/m^3 is the particle density in control volume sample n_c is number of particles in cold section i. e. from b-c-d-e-b at the center of the coil within control volume V_c.n_h is the number of particles in hot section i.e. from a-b-e-f-a at the center of the coil within control volume V_h. B_c is the maximum usable flux density available at the control volume of the center of the coil around the cold chamber. Whereas B_h is maximum usable flux density available at control volume of center of the coil around hot chamber. B_c field is at 45^o with the axis of coil where as similarly B_h field is also at 45^o with the axis of coil. n_s is number of particles in the center core of the coil taken together as a cold core

and hot core i.e full control volume. Cross sectional Area of control volume is A_s which contains A_c and A_h cross sectional areas of the control volume sample in cold as well as hot chamber spaces at the center core of the coil.

Whereas $B_s(usable)=B_c(usable)+B_h(usable)$,

Where $B_s(usable)$ is maximum flux density at the center of the coil. While $B_h(usable)$ and $B_c(usable)$ is flux densities at hot and cold core in the center of the coil after taking most probable states of the particles in hot and cold core respectively. $B_c(usable) = B_p \times n_c$ in cold core and $B_h(usable) = B_p \times n_h$ in hot core. Whereas, the value is very low due to impact of higher temperature on particles. The temperature dependencies of magnetization of the ferrofluid are given by classical Langevin theory of paramagnetism and not much of hysteresis is given by such a system.

n_c number of particles (n_s /2) will be in the most probable state in the cold core area of coil under very high external magnetizing force. This is the source of differential magnetization which will be non zero and give rise to fluctuations as $B_c(usable)$.

$B_s(usable) = B_c(usable)$

$|\Delta\Phi|$ maximum usable = $B_s(usable) \times A_s/2$.

Particles are under Brownian relaxation[23,24] and are governed by equation (9).

$$\tau_B = \frac{3\eta V}{kT} \quad (12)$$

This τ_B , Brownian relaxation time is in the order of 10^{-6}sec for 21 nm particle. Therefore maximum value of induced emf can be shown as equation (13).

$$e = -N\frac{k\,\Delta\Phi}{\tau_B} \quad (13)$$

$$K = -\left(\frac{e}{N}\right).\tau_B.\frac{1}{\Delta\phi} \quad (14)$$

$$|K| = \left(\frac{e}{N}\right).\tau_B.\frac{1}{\Delta\phi_{max}} \quad (15)$$

Since,

$$\Delta\phi_m = B_{s\,useful}\,.A_s/2 \quad (16)$$

Where A_s is full cross sectional area of chamber at center of coil.

$$\Delta\phi_m = B_p\,.n_c.A_s/2 \quad (17)$$

Where B_p is flux density per particle, n_c is number of particles in sample at center of coil with cold core.

$$n_c = \frac{\mu M_s}{\bar{m}}$$

$$n_c.\bar{m} = Bc(usable) = \Delta\phi_m/A_c \quad (18)$$

$$n_c.M_{spo}.cos\theta = \Delta\phi_m/A_c \quad (19)$$

$$n_c.M_{sp}\left[1-0.3\left(\frac{T}{T_c}\right)^{1.2}\right].cos\theta = \Delta\phi_m/A_c \quad (20)$$

$$A_c.n_c.M_{sp}\left[1-0.3\left(\frac{T}{T_c}\right)^{1.2}\right].cos\theta = \Delta\phi_m \quad (21)$$

Using equation-13 and replacing $\Delta\phi_{max}$

$$|K| = \left(\frac{e}{N}\right).\tau_B.\frac{1}{Ac.n_c.M_{sp}\left[1-0.3\left(\frac{T}{T_c}\right)^{1.2}\right].cos\theta} \quad (22)$$

Let us define a and b such that,

$$a = \frac{1}{N.Ac.n_c.cos\theta} \quad (23)$$

$$b = \frac{\tau_B}{M_{sp}} \quad (24)$$

$$\bar{m} = M_d\,.V = M_{sp}.cos\theta$$

Where M_d is the domain magnetization of bulk material, N is the number of turns of the coil and and τ_B is of the order of 10^{-6} sec.

a = 3.862 x 10^{-18} (1/m^2)

b = 4.705 x 10^{11} (Sec-m/A)

$$e = |K|.\frac{\left[1-0.3\left(\frac{T}{T_c}\right)^{1.2}\right]}{a.b} \text{ Volts} \quad (25)$$

Where, |k| is the coefficient of flux linkage with the coil. The measured value of generated emf was 800 µV at temperature of 318K. Negative sign of emf is only for direction convention. Experimentally observed value of |k| was 1.6 x 10^{-9} at temperature of 318K. Values of |k| at different temperatures are depicted in Fig-6.

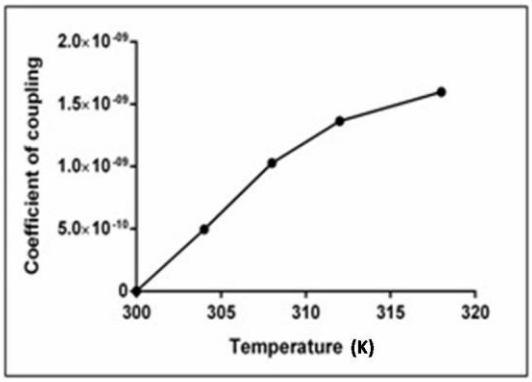

Figure 6. Effect of temperature on coefficient of coupling |k|

5.2 **Discussion on transportation of materials through channel**

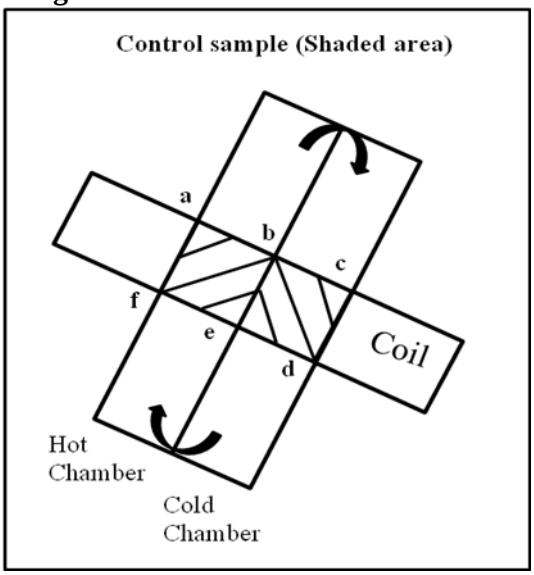

Figure 7. Showing control sample in shaded area

Considering control volume a-b-e-f-a in Fig-7, whereas the Raynold transportation of mass into control volume is analysed and given in equation- 26. For the purpose of system analysis on control volume, we must apply equations to a specific region rather than to individual masses. Reynolds transport theorem is applicable here. Consider a fixed control volume a-b-e-f-a with an arbitrary flow pattern. In general, each differential area *dA* of surface of inflow and out flow may have a different velocity *V* with a different angle θ with the normal to *dA*. One can find in flow volume of $(VAcos\theta)_{in}dt$ and outflow volume of $(VAcos\theta)_{out}dt$. Whereas the ferrofluid is assumed as an incompressible fluid and there is no accumulation of mass into any of the control volume. The flow will get developed slowly due to the heat flow at hot chamber and required to reach at control volume of hot chamber. For the system shown in Fig-7, an instantaneous change of B_{sys} in the system is sum of the change within control volume plus the outflow and minus the inflow. A_{in} and A_{out} are the cross sectional areas in the control volume in hot chamber. Whereas, integral CV and CS refer to control volume and control surface respectively; ρ is the density of ferrofluid and β is related to unit mass parameter. V_{olhc} control volume of hot chamber such that $\beta = dB/dm$ be the intensive value of the amount B per unit mass in any small element of the fluid.

A change within the control volume in hot chamber a-b-e-f-a is given by

$$\frac{\delta}{\delta t}\left(\int_{CV}\beta\rho dVolhc\right)$$

Outflow of β from the above control volume side a-b is given by

$$\int_{CS}\beta\rho V cos\theta dA_{out}$$

Inflow from same control volume is from side e-f

$$\int_{CS}\beta\rho V cos\theta dA_{in}$$

The Raynold transportation equation for control volume a-b-e-f-a in hot chamber is then given by -:

$$\frac{d}{dt}(B_{sys})\frac{\delta}{\delta t}\left(\int_{CV}\beta\rho d\text{Volhc}\right)+ \int_{CS}\beta\rho V\cos\theta\, dA_{out}-\int_{CS}\beta\rho V\cos\theta\, dA_{in} \quad (26)$$

Under certain circumstances, $m_{sys} = constant$. As the fluid is incompressible and there is no accumulation of mass within control volume under question, therefore differential volume is zero.

$$\frac{dm_{sys}}{dt} = 0 \quad (27)$$

Similar analysis can be carried out for control volume at cold chamber b-c-d-e-b also.

The maximum efficiency of such systems depends only on the temperature under test. T_H is a temperature input from copper plate of hot chamber and the temperature of the cold chamber is T_C. The maximum efficiency is given by

$$Efficiency = \left(1-\frac{T_c}{T_H}\right)\text{x}100\% \text{ .=5.66\%} \quad (28)$$

The actual efficiency is defined as -:

$$Efficiency = \frac{W}{Q_H}\text{x}100\% \quad (29)$$

Where, W is the work done by the heat input on sample and by the environment and Q_H is the heat extracted from the test cell. At the beginning of the cycle, the ferrofluid is held at a constant temperature of about 300 K. Work is done on the ferrofluid system and heat is exhausted to the cold reservoir. Initially, an internal energy of the system does not change since the temperature does not change. According to the First Law of Thermodynamics, $\Delta U = Q - W$ where Q is the heat added to the system and W is the work done by the system. In the second part of the cycle, heat is added to the system causing the ferrofluid colloidal to push the mass material slowly. Under magnetic field the material gets magnetically polarized and Brownian motion gets restricted giving rise to a differential magnetization. This differential magnetization of a control volume of hot and cold chamber will fluctuate more and more due to temperature rising and giving rise to emf generation in the coil.

VI. CONCLUSION

From the final equation of coefficient of coupling, |k| is very low. An unbalanced differential magnetic flux densities of these chambers taken in combination will give however small but non zero value of |k|.

It is observed that increase in emf with temperature shows an average rate of 44.4 µV/K. This generated emf is obtained after a certain time lapse, as it takes a while for heating the ferrofluid at the hot chamber for getting differential flux linkage. Generated emf will be measurable under the high value load impedances only. The order of load impedances required is in Mega Ohms.

ACKNOWLEDGEMENTS

One of the authors gratefully acknowledges Institute of Chemical Technology, Mumbai, India and Instrumentation Lab, Delphi Powers Pvt Ltd Pune, India for the help in research and instrumentation.

REFERENCES

Journal Papers:

[1] J.M. Renno, M.F. Daqaq, D.J. Inman, On the optimal energy harvesting from a vibration source, *J. Sound Vib. 320 (2009) 386–405. doi:10.1016/j.jsv.2008.07.029*.

[2] X. Cao, W.-J. Chiang, Y.-C. King, Y.-K. Lee, Electromagnetic Energy Harvesting Circuit With Feed forward and Feedback DC ndash;DC PWM Boost Converter for Vibration Power Generator System, *IEEE Trans. Power Electron.* 22 (2007) 679–685. doi:10.1109/TPEL.2006.890009.

[3] S.F. Medeiros, A.M. Santos, H. Fessi, A. Elaissari, Stimuli-responsive magnetic particles for biomedical applications, *Int. J. Pharm. 403 (2011) 139–161. doi:10.1016/j.ijpharm.2010.10.011*.

[4] S. Odenbach, Colloidal Magnetic Fluids: Basics, Development and Application of Ferrofluids, *Springer, 2009*.

[5] R. Jurgons, C. Seliger, A. Hilpert, L. Trahms, S. Odenbach, C. Alexiou, Drug loaded magnetic nanoparticles for cancer therapy, *J. Phys. Condens. Matter. 18 (2006) S2893. doi:10.1088/0953-8984/18/38/S24*.

[6] A.S. Lübbe, C. Alexiou, C. Bergemann, Clinical Applications of Magnetic Drug Targeting, *J. Surg. Res. 95 (2001) 200–206. doi:10.1006/jsre.2000.6030*.

[7] A. Candiani, M. Konstantaki, W. Margulis, S. Pissadakis, A spectrally tunable microstructured optical fibre Bragg grating utilizing an infiltrated ferrofluid, *Opt. Express. 18 (2010) 24654. doi:10.1364/OE.18.024654*.

[8] L. Martinez, F. Cecelja, R. Rakowski, A novel magneto-optic ferrofluid material for sensor applications, Sens. Actuators *Phys. 123–124 (2005)438–443. doi:10.1016/j.sna.2005.05.003*.

[9] R. Arulmurugan, G. Vaidyanathan, S. Sendhilnathan, B. Jeyadevan, Mn–Zn ferrite nanoparticles for ferrofluid preparation: Study on thermal–magnetic properties, *J. Magn. Magn. Mater. 298 (2006) 83–94. doi:10.1016/j.jmmm.2005.03.002*.

[10] T.-Y. Liu, S.-H. Hu, S.-H. Hu, S.-P. Tsai, S.-Y. Chen, Preparation and characterization of thermal-sensitive ferrofluids for drug delivery application, *J. Magn. Magn. Mater. 310 (2007)2850–2852. doi:10.1016/j.jmmm.2006.11.129*.

[11] Y.S. Kim, Analysis of Electromotive Force Characteristics for Electromagnetic Energy Harvester using Ferrofluid, *J. Magn. 20 (2015)252–257. doi:10.4283/JMAG.2015.20.3.252*.

[12] A.A. Kubasov, Electromotive force generation due to ferrofluid motion, *J. Magn. Magn. Mater. 173 (1997) 15–19. doi:10.1016/S0304-8853(97)00146-7*.

[13] D.K. Kim, M. Mikhaylova, Y. Zhang, M. Muhammed, Protective Coating of Superparamagnetic Iron Oxide Nanoparticles, *Chem. Mater. 15 (2003) 1617–1627. doi:10.1021/cm021349j*.

[14] I. Martínez-Mera, M.E. Espinosa-Pesqueira, R. Pérez-Hernández, J. Arenas-Alatorre, Synthesis of magnetite (Fe3O4) nanoparticles without surfactants at room temperature, *Mater. Lett. 61 (2007) 4447–4451. doi:10.1016/j.matlet.2007.02.018*.

[15] E. Hee Kim, H. Sook Lee, B. Kook Kwak, B.-K. Kim, Synthesis of ferrofluid with magnetic nanoparticles by sonochemical method for MRI contrast agent, *J. Magn. Magn. Mater. 289 (2005) 328–330. doi:10.1016/j.jmmm.2004.11.093*.

[16] A. Ryskin, H. Pleiner, Influence of a magnetic field on the Soret-effect-dominated thermal convection in ferrofluids, *Phys. Rev. E. 69 (2004) 046301. doi:10.1103/PhysRevE.69.046301*.

[17] M.I. Shliomis, M. Souhar, Self-oscillatory convection caused by the Soret effect, Europhys. *Lett. EPL. 49 (2000) 55–61. doi:10.1209/epl/i2000-00119-4*.

[18] R. Idris, I. Hashim, Effects of controller and cubic temperature profile on onset of Bénard–Marangoni convection in ferrofluid, *Int. Commun. Heat Mass Transf. 37 (2010) 624–628*.
doi:10.1016/ j.icheatmasstransfer.2009.11.015.

[19] I.S. Shivakumara, N. Rudraiah, C.E. Nanjundappa, Effect of non-uniform basic

temperature gradient on Rayleigh–Benard–Marangoni convection in ferrofluids, *J. Magn. Magn. Mater. 248 (2002) 379–395. doi:10.1016/S0304-8853(02)00151-8*.

[20] R.A. Ortega, T.D. Giorgio, A mathematical model of superparamagnetic iron oxide nanoparticle magnetic behavior to guide the design of novel nanomaterials, *J. Nanoparticle Res. 14 (2012). doi:10.1007/s11051-012-1282-x*.

[21] G.I. Barinov, S.S. Aplesnin, Change in the critical exponent of magnetization in maghemite in the temperature range of the structural phase transition, *Phys. Solid State. 48 (2006) 84–87. doi:10.1134/S1063783406010173*.

[22] P. Jönsson, T. Jonsson, J.L. Garcıa-Palacios, P. Svedlindh, Nonlinear dynamic susceptibilities of interacting and noninteracting magnetic nanoparticles, *J. Magn. Magn. Mater. 222 (2000) 219–226. http://www.sciencedirect.com/science/article/pii/S0304885300005576 (accessed February 20, 2016)*.

[23] B. Fischer, B. Huke, M. Lücke, R. Hempelmann, Brownian relaxation of magnetic colloids, *J. Magn. Magn. Mater. 289 (2005)74–77. doi:10.1016/j.jmmm.2004.11.021*.

[24] R. Kötitz, P.C. Fannin, L. Trahms, Time domain study of Brownian and Néel relaxation in ferrofluids, *J. Magn. Magn. Mater. 149 (1995) 42–46. doi:10.1016/0304-8853(95)00333-9*.

Chapters in Books:

[25] K.H.J.Buschow, *volume 2, Handbook of Magnetic Materials.[2015]* .

[26] R. C. O´Handley, *section 3, Handbook of Magnetic Materials. [2000]*.

Proceeding Papers:

[27] S D Kemkar, H S Mahajan, M. Vaidya, Ferrofluid based optical fiber switch, *AIP Conference Proceedings 2012, Vol 1447, 512-522*.

[28] S D Kemkar, 2D Fractional microcontroller based tilt measurement system using ferrofluid, *Sensor-13, 13th National Seminar March 3-5 2008, C-8-1*.

[29] S D Kemkar, H S Mahajan, Milind Vaidya, Selective Switching action in optical fiber using fe3O4 based ferrofluid. *Proceedings of International Conference in advances in computer and communication technology-ACCT 2012, 14-15*.

[30] S D Kemkar, Design and Development of tilt angle measurement based on microcontroller system using ferrofluid, *52 DAE Solid State physics Symposium, Mysore, 2007*.

[31] V.A Bambole, S D Kemkar, H S Mahajan, S K Gupta, Electronic devices based on non linear characteristics of electron beam irradiated HPMC + PPy blends, *National conference on advanced materials and technologies (NCAMDT-2008), Feb 20-22, 2008, Sri Venkateshwara University, pg 49-50*.

[32] V A Bambole, H S Mahajan, S K Gupta, S P Koiry, S D Kemkar, Study of variation of conductivity of electron beam irradiated HPMC= PPy films with dose rate , National conference on advanced materials and technologies (NCAMDT-2008), Feb 20-22, 2008, Sri Venkateshwara University, *pg. 161*.